



Versatile genetic paintbrushes: Brainbow technologies

Benjamin Richier and Iris Salecker*

Advances in labeling technologies are instrumental to study the developmental mechanisms that control organ formation and function at the cellular level. Until recently, genetic tools relied on the expression of single markers to visualize individual cells or lineages in developing and adult animals. Exploiting the expanding color palette of fluorescent proteins and the power of site-specific recombinases in rearranging DNA fragments, the development of Brainbow strategies in mice made it possible to stochastically label many cells in different colors within the same sample. Over the past years, these pioneering approaches have been adapted for other experimental model organisms, including *Drosophila melanogaster*, zebrafish, and chicken. Balancing the distinct requirements of single cell and clonal analyses, adjustments were made that both enhance and expand the functionality of these tools. Multicolor cell labeling techniques have been successfully applied in studies analyzing the cellular components of neural circuits and other tissues, and the compositions and interactions of lineages. While being continuously refined, Brainbow technologies have thus found a firm place in the genetic toolboxes of developmental and neurobiologists. © 2014 The Authors. *WIREs Developmental Biology* published by Wiley Periodicals, Inc.

How to cite this article:

WIREs Dev Biol 2015, 4:161–180. doi: 10.1002/wdev.166

INTRODUCTION

To address fundamental questions in developmental biology, regardless of the organ, tissue, or model organism, it is essential to visualize cell types of interest. This must be accomplished, as cells divide, migrate, or acquire their mature shapes during normal development and upon functional perturbations. Similarly, detailed information about the morphology and connectivity of neurons within neural circuits is a prerequisite for neurobiological studies aiming at understanding brain function. Ideally in morphological studies, individual cells within genetically defined populations are labeled sparsely within a

sample (Figure 1(a)). The targeting of cells critically depends on the enhancers used to drive expression of a visible marker. These may be active in a given cell subtype, but are rarely specific to single cells. Mosaic approaches, combined with cell type-specific enhancers, have thus become instrumental to facilitate single cell labeling.¹ However, a drawback is that surrounding cells are generally not visible. Consequently, many independent samples are required to assemble a likely incomplete picture of the environment and occurring cell–cell interactions. To assess lineages, one can take advantage of the fact that progeny continue to express the same stable inheritable marker as the precursor, from which they are derived (Figure 1(b)). However, this may limit anatomical studies if a single reporter is used and cell morphology can no longer be unambiguously determined. This can occur when cells form clusters, are born in the same narrow time window or develop extensive overlapping processes.

*Correspondence to: isaleck@nimr.mrc.ac.uk

MRC National Institute for Medical Research, Division of Molecular Neurobiology, London, UK

Conflict of interest: The authors have declared no conflicts of interest for this article.

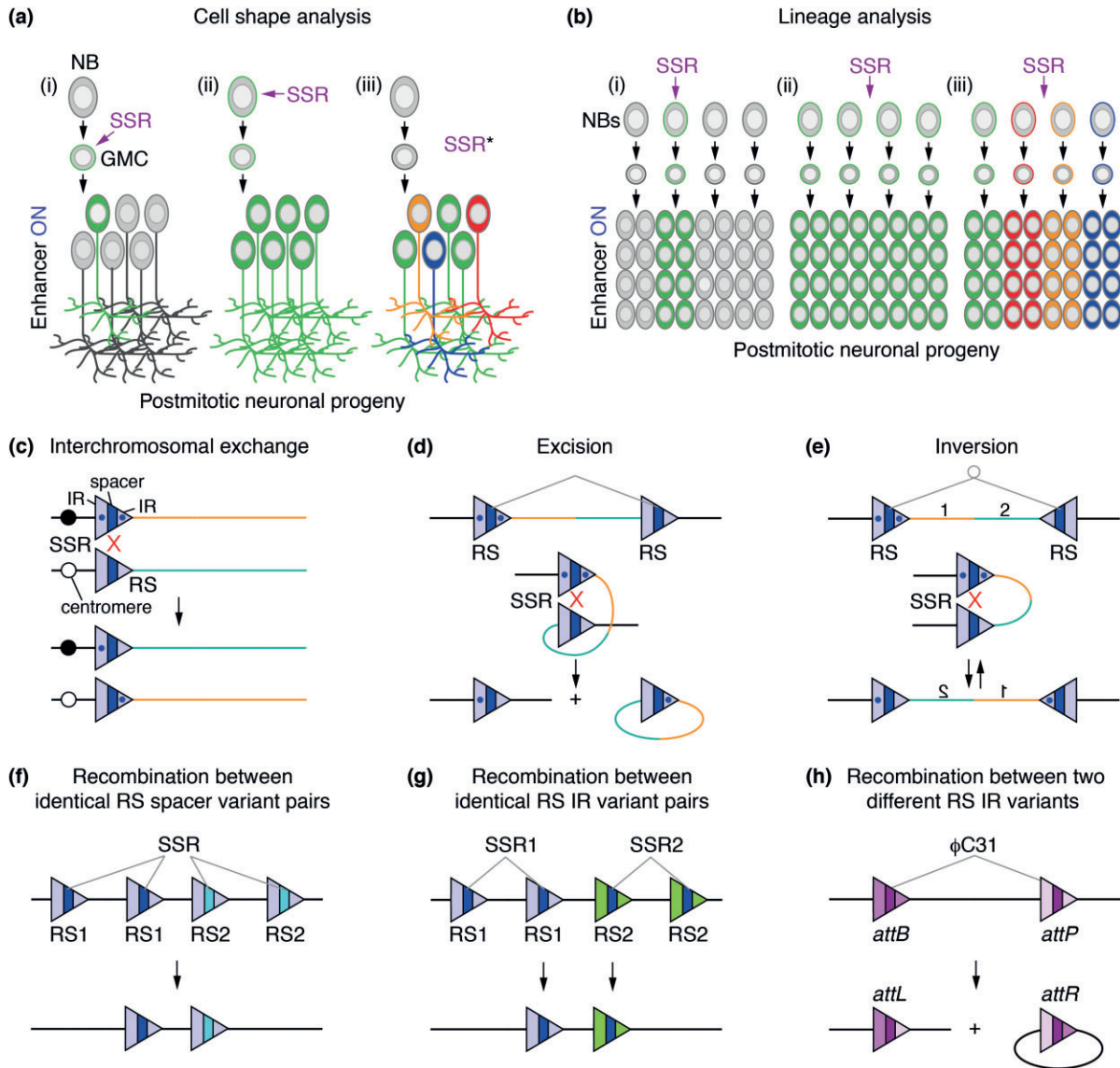


FIGURE 1 | Brainbow techniques take advantage of DNA rearrangements mediated by site-specific recombinases. (a, b) Two aims of multicolor labeling approaches are illustrated in the developing *Drosophila* nervous system, but also apply to other cell types and tissues. Neural stem cell equivalents, the neuroblasts (NBs), self-renew and produce ganglion mother cells (GMCs). These divide to produce postmitotic neuronal progeny, which can be visualized with specific enhancers (ON) driving the expression of reporters. (a) Anatomical studies of overlapping neuron branches require sparse labeling of individual cells. In mosaic approaches, single (i) or lineage-related cells (ii) can be visualized, if recombination events by site-specific recombinases (SSR) are triggered in GMCs or NBs, respectively. Unlike monochrome reporters (ii), sparse multicolor labeling enables the tracing of several neurons in the same sample (iii), even if they are lineage-related or targeted by the same enhancer. SSR*, multicolor labeling can be achieved by recombinase activity in precursors or progeny. (b) Lineage analyses require comprehensive labeling of entire sets of progeny. Activity of SSRs in one precursor allows the labeling of a single clone (i). If a single reporter is used, progeny of multiple lineages can no longer be discerned (ii). Multicolor labeling makes it possible to study several lineages in the same sample (iii). Prior to enhancer activation, FPs are indicated as colored outlines of cells; full expression is indicated by filled cells. (c–h) Cre or FLP SSRs catalyze specific recombination events between pairs of target recombination sites (RS). Each RS consists of two inverted repeats (IR) and a spacer, determining RS directionality. (c) Two RS sites with the same orientation positioned *in trans* trigger the exchange of sequences between homologous chromosome arms. This configuration is used for mosaic approaches, such as MARCM.⁶³ (d) SSRs mediate excision of DNA fragments between RS pairs with the same orientation and positioned *in cis*. (e) SSRs catalyze reversible inversions of DNA fragments located between RS pairs with opposite orientations. (f) SSRs mediate recombination between identical pairs of heterospecific site variants that differ in the spacer sequence (blue and cyan). (g) SSR variants are specific for target site pairs with distinct IR sequences (light blue, green). (h) ϕ C31 mediates irreversible recombination events between *attB* and *attP* sites, characterized by distinct imperfect IR sequences, to generate new *attL* and *attR* sites.

Moreover, to uncover relative contributions of cell lineages, growth rates, or competitive interactions, the ability to track the coordinated behavior of multiple independent clones in the same sample is central. This is particularly beneficial for studies focusing on organ morphogenesis, where comprehensive labeling of proliferating precursors and their offspring is preferred. Labeling with multiple markers thus offers a clear way forward to simultaneously visualize numerous individual cells or complete lineages in the same sample with high resolution (Figure 1(a) and (b)).

Because of the enormous complexity of neuronal shapes and connections in the brain, it was perhaps not unexpected that the strongest need for a genetic multicolor labeling tool was felt by neurobiologists. In 2007, Livet et al.² pioneered a landmark technique to label neurons in a mosaic of many different colors by stochastic and combinatorial expression of a restricted set of fluorescent proteins (FPs) in the mouse brain. This approach was named ‘Brainbow’ because of its primary purpose to map neuronal connectivity. However, it quickly became clear that this technology was also essential for studies in other tissues and model organisms. Thus, over the past years, Brainbow approaches have steadily evolved to circumvent initial limitations and to extend their functionality in response to the requirements of different fields. This review introduces the key genetic building blocks employed by multicolor labeling methods. It then provides a guide to currently available technologies in different model organisms for studies in the nervous system and beyond.

THE BUILDING BLOCKS

FPs as Imaging Probes

Brainbow approaches (Table 1) would not have been possible without the development of spectrally separable FPs as genetically encoded visible markers and the progress in imaging technologies. The founding member of FPs, Green fluorescent protein (GFP), was discovered in jellyfish *Aequorea victoria* as partner of the bioluminescent protein Aequorin in 1962.¹⁹ It was successfully cloned for transgenic expression in prokaryotic and eukaryotic cells in 1994.²⁰ GFP can be excited with blue light to emit a green fluorescence signal. The subsequent isolation of naturally occurring FPs from other hydrozoan species,²¹ anthozoan corals, such as *Clavularia* sp.,²² *Discosoma* sp.²³ and *Fungia concinna*,^{24,25} or the sea anemone *Entacmaea quadricolor*,²⁶ as well as systematic bioengineering approaches expanded the color palette ranging from blue to red (Table 2). For instance,

jellyfish-derived GFP was modified to create blue, cyan, and yellow FPs,^{31–33,37} while *Discosoma*-derived DsRed was used to generate orange, red, and far-red variants.^{41,39} Furthermore, because natural FPs have the basic property of forming dimers or tetramers, mutations were introduced that produce functional monomeric versions.⁴⁰ Additional amino acid changes increased the brightness, maturation rate and photostability, or decreased pH and temperature sensitivity.^{39,50}

FP emission signals can be collected directly to visualize expression in living or fixed cells by confocal laser scanning microscopes that are equipped with different laser lines and highly sensitive detection devices able to perform spectral separations of narrow wavelength bands. Some FPs are also compatible with multiphoton excitation methods to facilitate imaging of thick samples.⁵¹ Tissue-clearing technologies, such as *Scale*⁵² and *CLARITY*⁵³ further increase image resolution. Moreover, because proteins from jellyfish, coral, and sea anemone species are antigenically distinct and FPs are easily epitope-tagged, expression can also be detected by immunofluorescence labeling using primary antibodies directed either against the FP variant or tags.^{3,4,16} In all cases, imaging software is used to assign specific colors (e.g., green, yellow, red, or blue) to signals collected in different channels. These can—but do not need to—match the emission spectra of FPs or fluorophore-coupled secondary antibodies. Mixed colors are achieved by the overlay of images acquired in each channel.

Unmodified FPs accumulate in the somatic cytoplasm and only partially spread into cellular processes. For studies in the nervous system, where extensive dendritic and axonal arbors have to be visualized, it is thus helpful to use membrane anchors. In Brainbow technologies, these include a mouse Cd8a sequence,^{4,42,43} a farnesylation signal from Ras,^{10,16,45,54} a myristoylation-palmitoylation (myr-palm) sequence from Lyn kinase^{4,36} and a palmitoylation sequence from Gap43.^{2,6–8,17,46} The GRASP approach (GFP reconstitution across synaptic partners) employs a truncated version of the human T cell protein Cd4 as a membrane-tether of GFP fragments in worms and flies.^{55,56} This anchor has also successfully been used to generate membrane-bound versions of tdTomato,⁵⁷ and thus could serve as a valuable alternative in future Brainbow constructs. Additionally, FPs are targeted to the nucleus using a nuclear localization signal or Histone-2A and 2B sequences.^{2,8–10,15,17,47,48} Finally, subcellular targeting of FPs to mitochondria is achieved with a sequence from the human cytochrome c oxidase subunit 8 (COX8)^{17,49} (Table 2).

TABLE 1 | Summary of Described Multicolor Labeling Techniques

	Tool name	Strategy	Recomb.	E/P	Stop	FP1/ FP2/ FP3/ FP4 + subcellular localization signal and epitope tags	Ref.
mouse	<i>Brainbow-1.0</i>	1 (L)	Cre	<i>Thy1</i>	no	dTomato/ mCerulean/ mEYFP/ -	2
	<i>Brainbow-1.1</i>	1 (M)	Cre	<i>Thy1</i>	no	mKO/ p mCherry/ p mEYFP/ p mCerulean	2
	<i>Brainbow-2.0</i>	2	Cre	<i>Thy1</i>	no	tdimer2/ p ECFP/ -/ -	2
	<i>Brainbow-2.1</i>	2 (R)	Cre	<i>Thy1</i>	no	hrGFP II nls / mEYFP/ tdimer2/ p mCerulean	2
<i>Drosophila</i>	<i>dBrainbow</i>	1	Cre	10xUAS	yes	EGFP ^{V5} / EBFP2 ^{H2A} / mKO2 ^{myc} / -	3
	<i>Flybow-1.0</i>	2	mFLP5	10xUAS	no	cd8 mCherry/ cd8 mCerulean ^{V5} / -/ -	4
	<i>Flybow-1.1</i>	2	mFLP5	10xUAS	no	cd8 EGFP/ mp mCitrine/ cd8 mCherry/ cd8 mCerulean ^{V5}	4
	<i>Flybow-2.0</i>	2	mFLP5	10xUAS	yes	cd8 EGFP/ mp mCitrine/ cd8 mCherry/ cd8 mCerulean ^{V5}	4
	<i>Flybow-1.0B</i>	2	mFLP5	10xUAS	no	cd8 mCherry/ mp mTurquoise/ -/ -	5
	<i>Flybow-1.1B</i>	2	mFLP5	10xUAS	no	cd8 EGFP/ mp mCitrine/ cd8 mCherry/ mp mTurquoise	5
	<i>Flybow-2.0B</i>	2	mFLP5	10xUAS	yes	cd8 EGFP/ mp mCitrine/ cd8 mCherry/ mp mTurquoise	5
	<i>UAS-Brainbow</i>	1 (M)	Cre	5xUAS	no	mKO/ p mCherry/ p mEYFP/ p mCerulean	6
	<i>LOLLIbow</i>	1 (M)	Cre	5xUAS	no	mKO/ p mCherry/ p mEYFP/ p mCerulean	7
	<i>UAS-Brainbow2.1R-2</i>	2 (R)	Cre	5xUAS	no	hrGFP II nls/ mEYFP/ tdimer2/ p mCerulean	8
	<i>TIE-DYE</i>	-	FLP	<i>act, ubi, UAS</i>	yes	three separate transgenes: <i>act>> lacZ nls, ubi>>EGFP nls, act>>Gal4, UAS-H2A-mRFP1</i>	9
	<i>Raepli-NLS</i> <i>Raepli-CAAX</i>	1	φC31-self exc.	5xUAS/ <i>lexAop</i>	yes	E2-Orange nls/ mKate2 nls/ mTFP1 nls/ mTagBFP nls E2-Orange f/ mKate2 f/ mTFP1 f/ mTagBFP f	10
zebrafish	<i>zebrafish Brainbow</i>	1 (L)	Cre	<i>CMV</i>	no	dTomato/ mCerulean/ mEYFP/ -	11
	<i>βact2-Brainbow</i>	1 (L)	Cre	<i>βact2</i>	no	dTomato/ mCerulean/ mEYFP/ -	12
	<i>UAS-Brainbow-1.0L</i>	1 (L)	Cre	14xUAS	no	dTomato/ mCerulean/ mEYFP/ -	13
	<i>UAS-Zebrabow-V</i>	1 (L)	Cre	14xUAS	no	dTomato/ mCerulean/ mEYFP/ -	14
	<i>UAS-Zebrabow-B</i>	1 (L)	Cre	4xUAS ^{sr}	no	dTomato/ mCerulean/ mEYFP/ -	14
	<i>ubi-Zebrabow-S</i>	1 (L)	Cre	<i>ubi</i>	no	dTomato/ mCerulean/ mEYFP/ -	14
	<i>ubi-Zebrabow-M</i>	1 (L)	Cre	<i>ubi</i>	no	dTomato/ mCerulean/ mEYFP/ -	14
mouse (next generation)	<i>Confetti</i>	2 (R)	Cre	<i>CAG</i>	yes	hrGFP II nls/ mEYFP/ tdimer2/ p mCerulean	15
	<i>Brainbow-3.0</i>	1	Cre	<i>Thy1</i>	no	mOrange2 f/ EGFP f/ mKate2 f/ -	16
	<i>Brainbow-3.1</i>	1	Cre	<i>Thy1</i>	yes	mOrange2 f/EGFP f/ mKate2 f/ -	16
	<i>Brainbow-3.2</i>	1	Cre	<i>Thy1</i>	yes	mOrange2 f W/ EGFP f W/ mKate2 f W/ -	16
	<i>Autobow</i>	1	Cre - self exc.	<i>Thy1</i>	yes	mCerulean/ PhiYFP/ mKate2/ -	16
	<i>Flpbow-3.0</i>	1	Cre	<i>Thy1</i>	no	tdTomato/ PhiYFP/ ECFP/ -	16
	<i>Flpbow-3.1</i>	1	Cre	<i>Thy1</i>	yes	^S mOrange2 f W/ ^S EGFP f W/ ^S mKate2 f W/ -	16
mouse, chicken	<i>MAGIC markers</i> <i>Cytbow</i>	1	Cre	<i>CAG</i>	no ^a	H2B EBFP2/ tdTomato/ mCerulean or mTurquoise2/ mEYFP	17
	<i>Nucbow</i>	1	Cre	<i>CAG</i>	no ^a	H2B EBFP2/ H2B mEYFP/ H2B mCherry/ H2B mCerulean	17
	<i>Palmbow</i>	1	Cre	<i>CAG</i>	no ^a	H2B EBFP2/ p mCherry/ p mEYFP/ p mCerulean	17
	<i>Mitbow</i>	1	Cre	<i>CAG</i>	no ^a	H2B EBFP2/ mit mEYFP/ mit mCherry/ mit mCerulean	17
	<i>CLoNe</i> <i>pPB-STOP-cyXFP</i>	-	Cre	<i>CAG</i>	yes	EGFP, mT-Sapphire, mEYFP or mCherry	18
	<i>pPB-STOP-ncXFP</i>	-	Cre	<i>CAG</i>	yes	H2B EGFP, mT-Sapphire, mEYFP or mCherry	18
	<i>pPB-STOP-mbXFP</i>	-	Cre	<i>CAG</i>	yes	p EGFP, mT-Sapphire, mEYFP or mCherry	18

1, Brainbow-1, 2, Brainbow-2; *act*, *actin*; *CAG*, *chicken β-actin promoter with cytomegalovirus* enhancer; *CMV*, *cytomegalovirus* enhancer; *cy*, cytoplasmic; *d*, dimeric; E/P, enhancer/promoter; H2A, Histone-2A; H2B, Histone-2B; hrGFP II, humanized recombinant GFP II; f, farnesylation; mb, membrane-bound; mit, mitochondrial; m, monomeric; mKO, mKusabira Orange; mKO2, mKusabira Orange2; mp, myristoylation-palmitoylation; mT, monomeric Turbo; nc, nuclear; nls, nuclear localization signal; nr, non-repetitive; p, palmitoylation; self-exc., self excising; S, SUMOstar fusion; td, tandem dimer; *ubi*, *ubiquitin*; W, woodchuck hepatitis virus post-transcriptional regulatory element; ≫, symbol for *FRT*-flanked stop cassette.

^aOwing to its nuclear localization and UV-shifted emission, H2B EBFP functions similarly to a stop cassette.

TABLE 2 | Fluorescent Proteins and Subcellular Tags Used by Multicolor Labeling Techniques

Color	Fluorescent protein	Excitation peak (nm)	Emission peak (nm)	Species	Ref.
Blue - BFP	EBFP2	383	448	<i>Aequorea victoria</i>	27
	mTagBFP	399	456	<i>Entacmaea quadricolor</i>	28
Cyan - CFP	ECFP	433	476	<i>Aequorea victoria</i>	29,30
	mCerulean	433	475	<i>Aequorea victoria</i>	31
	mTurquoise	434	474	<i>Aequorea victoria</i>	32
	mTurquoise2	434	474	<i>Aequorea victoria</i>	33
	mTFP1	462	492	<i>Clavularia sp.</i>	22
Green - GFP	EGFP	488	507	<i>Aequorea victoria</i>	29,30
	hrGFP II	500	506	<i>Renilla reniformis</i>	2
	mT-Sapphire	399	511	<i>Aequorea victoria</i>	34,35
Yellow - YFP	mEYFP	515	528	<i>Aequorea victoria</i>	36
	mCitrine	516	529	<i>Aequorea victoria</i>	37
	PhiYFP	525	537	<i>Phialidium sp.</i>	21
Orange - OFP	E2-Orange	540	561	<i>Discosoma sp.</i>	38
	mKusabira Orange	548	559	<i>Fungia concinna</i>	24
	mOrange2	549	565	<i>Discosoma sp.</i>	39
	mKusabira Orange2	551	565	<i>Fungia concinna</i>	25
Red - RFP	tdimer2	552	579	<i>Discosoma sp.</i>	40
	dTomato	554	581	<i>Discosoma sp.</i>	41
	tdTomato	554	581	<i>Discosoma sp.</i>	41
	mRFP1	584	607	<i>Discosoma sp.</i>	40
Red - RFP	mCherry	587	610	<i>Discosoma sp.</i>	41
Red - RFP	mKate2	588	633	<i>Entacmaea quadricolor</i>	26
Localization	Type	Details		Ref.	
Membrane	cd8	amino acids 1-220 from mouse CD8a		42,43	
	farnesylation (f)	20 C-terminal amino acids of human c-HA-RAS including CAAX motif and palmitoylation sites		44,45	
	myristoylation-palmitoylation (myr-palm, mp)	amino acids 1-16 from Lyn kinase		36	
	palmitoylation (palm, p)	amino acids 1-20 of zebrafish Gap43		46	
Nucleus	nuclear localization signal (nls)	1 or 3 nuclear localization signals from SV40 large T antigen		10,47	
	Histone-2A (H2A)	coding sequence of <i>Drosophila</i> Histone-2A		48	
	Histone-2B (H2B)	human Histone-2B sequences		17,18	
Mitochondria	mitochondrial targeting signal (mit)	amino acids 1-31 of human cytochrome c oxidase subunit 8 (COX8)		17,49	

d, dimer; hrGFP II, humanized recombinant GFP II; m, monomeric; mT, monomeric Turbo; t, tandem; td, tandem dimer.

Control of Transgene Expression

Reporter expression is achieved by tissue- or cell type-specific enhancer elements. Multicolor cell labeling approaches in vertebrate model organisms rely on the direct transcriptional activation by neuron-specific or ubiquitous enhancers (Table 1). By contrast, *Drosophila* transgenes benefit from the flexibility offered by binary expression systems. In particular, the

Gal4/UAS system has become a corner stone of genetic studies in flies.⁵⁸ In this approach, the yeast-derived transcription factor Gal4, when expressed under the control of a specific enhancer, binds tandem *Upstream Activating Sequences* (UAS), which activate transcription of genes including those encoding visible markers. In *Drosophila*, a large number of Gal4 driver lines has been generated that show specific activities in

TABLE 3 | Site-Specific Recombination Systems Used by Multicolor Labeling Techniques

Recomb.	Site	Sequence →	Variant	Ref.
Cre	<i>loxP</i>	ATAACTTCGTATA ATGTATGC TATACGAAGTTAT		72
	<i>lox2272</i>	ATAACTTCGTATA AAGTATCC TATACGAAGTTAT	spacer	72
	<i>loxN</i>	ATAACTTCGTATA AGGTATAC TATACGAAGTTAT	spacer	2
	<i>lox5171</i>	ATAACTTCGTATA ATGTGTAC TATACGAAGTTAT	spacer	72
FLP	<i>FRT</i>	GAAGTTCCTATAC TTTCTAGA GAATAGGAACTTC		73,74
	<i>FRT3^a</i>	GAAGTTCCTATAC TATTTGAA GAATAGGAACTTC	spacer	16,75,76
	<i>FRT5T2</i>	GAAGTTCCTATAC CTCTAGA GAATAGGAACTTC	spacer	16,73
	<i>FRT545</i>	GAAGTTCCTATAC TTTTAGA GAATAGGAACTTC	spacer	16,73
mFLP5	<i>mFRT71</i>	GAAGTTCCTATAC TTTCTAGA GAATAGAACTTC	inverted repeat	4,77
φC31	<i>attP^b</i>	CCCCAACTGGGGTAACCT TTG AGTTCTCTCAGTTGGGGG		78,79
	<i>attB^b</i>	GTGCCAGGGCGTGCC TTG GGCTCCCCGGGCGC		
Model	Recombinase source	Activity	Ref.	
mouse	<i>CAG-CreERT2</i> (synonym: <i>CAG-CreERTM</i>)	ubiquitous, tamoxifen-inducible	2,16,17	
	<i>Chx10-Cre</i>	retina	2	
	<i>Emx1-Cre</i>	cortex	2	
	<i>Islet1-Cre</i>	retina, basal ganglia, neuromuscular junctions	2,16	
	<i>L7-Cre</i>	Purkinje cells in cerebellum	16	
	<i>Pax6a-Cre</i>	retina	2	
	<i>PV-Cre</i>	Parvalbumin-expressing neurons	16	
	<i>Cre</i> integrated in <i>Autobow</i> transgenes	postmitotic neurons, dependent on <i>Thy1</i> activity	16	
	<i>Ah-Cre</i> (controlled by <i>cytochrome P450</i> enhancer)	β-naphthoflavone-inducible	15	
	<i>Lgr5-EGFP-Ires-CreERT2</i>	intestinal stem cells, tamoxifen-inducible	15	
	<i>Wnt-FLPe</i>	dorsal striatum and other CNS areas	16	
	<i>Tbr2-Cre</i>	intermediate progenitors in SVZ	18	
	mouse, chicken EP	<i>se-Cre</i> (CAG controlled vector)	ubiquitous, self-excising Cre	17
<i>ERT2CreERT2</i> (CAG controlled vector)		ubiquitous, tamoxifen-inducible, no background activity in absence of tamoxifen	17	
<i>CAG-Cre</i> vector		ubiquitous	18	
<i>Emx2-Cre</i> vector		neocortical radial glia	18	
<i>Dlx1/2-Cre</i> vector		subpallial forebrain progenitors	18	
Drosophila	<i>hsp70.Mos1-Cre</i>	ubiquitous, constitutively active	80	
	"split-Cre": <i>UAS-CIBN::Cre-N, UAS-CRY2::Cre-C</i>	Gal4-dependent, light-inducible	7	
	<i>hs-Cre-HA</i>	ubiquitous, temperature-inducible, some basal activity	8	
	<i>hs-FLP^c</i>	ubiquitous, temperature-inducible, medium efficiency	68,81	
	<i>hs-FLP¹²²</i> (synonym: <i>hsp70-FLPI^c</i>)	ubiquitous, temperature-inducible, high efficiency	82	
	<i>UAS-FLP</i>	Gal4-dependent	83	
	<i>hs-mFLP5</i>	ubiquitous, temperature-inducible	4,77	
	<i>φC31</i> integrated in <i>Raepli</i> transgenes	dependent on heat or Gal4 induced FLP mediated excision of stop cassette, controlled by <i>hsp70</i> or <i>UAS</i>	10	
zebrafish	<i>hsp-Cre</i>	ubiquitous, temperature-inducible	11,14	
	<i>hsp70l-Cre</i>	ubiquitous, temperature-inducible, low basal activity	13,84	
	<i>ubi-CreER</i>	ubiquitous, tamoxifen-inducible	14	
	<i>pax2a-CreER</i>	diencephalon, tamoxifen-inducible	14	
	<i>cmle2-CreER</i>	cardiomyocytes, tamoxifen-inducible	12,14	

CAG, chicken β-actin promoter with cytomegalovirus enhancer; EP, electroporation; *hs*, heat shock; PV, parvalbumin; *se*, self-excising; SVZ, subventricular zone; *ubi*, ubiquitin. Sequences highlighted in blue indicate inverted repeats. Base pair changes in site variants are shown in red. The arrow indicates orientations of recombination sites based on the spacer sequence. Recombination site sequence orientations are presented as reported in original studies.^{72,73} References for vertebrate Cre recombinases can be found within provided Brainbow technology publications.

^a*FRT3* is also known as *FRT3^{0,88}* or *FRT2*.

^bReported high efficiency minimal *attP* and *attB* sites recombine to create new *attR* and *attL* sites.

^cThe precise FLP protein sequence in these transgenes has not been determined. Nern et al.⁸⁵ recently reported that FLP variants with aspartic acid at amino acid residue 5 are 10 times more efficient compared to variants that contain glycine at this position.

different tissues and cell types during development and in adults. These can be enhancer trap insertions, as well as lines, in which Gal4 is expressed under the control of defined enhancer fragments.^{59–62} Further spatiotemporal control can be achieved by the Gal4 repressor Gal80.⁶³ When two different enhancers with activities in partially overlapping cell populations are used, expression of Gal4 is solely possible in the subgroup of cells that does not express Gal80. Moreover, a temperature-sensitive Gal80 variant can control expression in developmental time windows.⁶⁴ Other binary expression systems such as *LexA/lexAop* and *QF/QUAS* have recently been introduced as complementary approaches.^{65–67} These tools can be combined to enable independent manipulation of different cell types or to refine expression to a few or even single cell types in intersectional strategies.

Mosaic Expression with Site-Specific Recombinases

To facilitate controlled mosaic expression of visible markers in cells of interest, Brainbow technologies rely on a third set of genetic tools—the site-specific DNA recombinases. These mediate recombination between specific short DNA sequences by catalyzing strand cleavage, exchange and ligation.^{68–70} They are grouped into tyrosine or serine recombinases depending on the amino acid required for the catalytic reaction.⁷¹ Multicolor cell labeling approaches utilize most commonly the tyrosine recombinases Cre and FLP (Table 3). Cre is derived from the bacteriophage P1 and specifically recognizes *loxP* [*locus of cross-over (X) in P1*] sites, while FLP recombinases were isolated from *Saccharomyces cerevisiae* and bind to *FRT* (*FLP recombinase target*) sites. Both minimal *lox* and *FRT* sites consist of two 13-bp inverted repeats.^{69,72,73} These flank an asymmetric 8-bp spacer sequence, which confers directionality to the sites.⁷⁴ The relative positions and orientation of *lox* or *FRT* pairs determine the outcome of recombination events. When two identical sites are located on homologous chromosomes, interchromosomal recombination events can be triggered during cell divisions. In *Drosophila*, *FRT* sites positioned close to centromeres have been particularly useful for generating somatic clones that are homozygous for genes of interest, while all other cells in the animal are heterozygous⁷⁰ (Figure 1(c)). Intrachromosomal recombination events can lead either to excision of a DNA sequence positioned between *lox* or *FRT* pairs, when they have the same orientation, or inversion, when they have the opposite orientation^{69,86} (Figure 1(d) and (e)). Excisions constitute irreversible events because only one

functional site remains. By contrast, inversions are reversible because two functional sites are recreated.

While Cre can recognize several *lox* sites, which differ in the spacer sequence (e.g., *loxP*, *lox2272*, *lox5171*, and *loxN*),^{2,87} they solely mediate recombination events between identical spacer variant pairs. Similarly, FLP can distinguish *FRT* spacer variants (e.g., *FRT3*, *FRT5T2*, and *FRT545*)^{16,73,75,76} (Figure 1(f)). In addition, a FLP variant, mFLP5, shows high specificity for a modified site, *mFRT71*, characterized by sequence changes in the inverted repeats, and little to no cross-reactivity with canonical *FRT* sites^{4,77} (Figure 1(g)). Finally, new recombinases from different yeast species—KD, R, B2, and B3—were recently added to the genetic toolbox, which mediate recombination events of four distinct target sites.⁸⁵

Whereas most genetic approaches in vertebrates rely on Cre, this recombinase has found only limited applications in *Drosophila* for two reasons. First, initially generated Cre transgenes in *Drosophila* show constitutive activity that cannot readily be controlled in time or space.⁸⁰ Cre is therefore primarily used for manipulations where efficient excisions in many cells including the germ line are desired (e.g., Ref 88). Second, it shows toxicity in proliferating cells upon persistent over-expression likely due to chromosomal aberrations caused by recombination of pseudo *loxP* sites.⁸⁹ Because the lower efficiency of FLP is suitable for mosaic analysis experiments, this recombinase therefore has become the preferred tool for this type of genetic manipulations in flies.

φC31 integrase from the *Streptomyces* bacteriophage belongs to the family of serine recombinases.^{78,79} This enzyme catalyzes the unidirectional recombination between bacterial attachment (*attB*) sites, often positioned in plasmids, and phage attachment (*attP*) sites, serving as genomic landing sites. Recombination events are irreversible because the newly generated *attL* (Left) and *attR* (Right) sites are no longer recognized by the integrase (Figure 1(h)). In *Drosophila*, this system is used for controlled genomic integration of DNA sequences,^{90,91} cassette exchange,⁹² or fragment excisions.¹⁰

The regulation of recombinase expression is used to influence the timing and frequency of events (Table 3). Importantly, this does not impact on the levels of markers because their expression is under the control of an independent enhancer. To transiently induce high expression in *Drosophila* or zebrafish, FLP and Cre recombinases are placed downstream of a heat shock promoter.^{14,68,80,82} In fish and mammals, temporal activation can also be achieved with the help

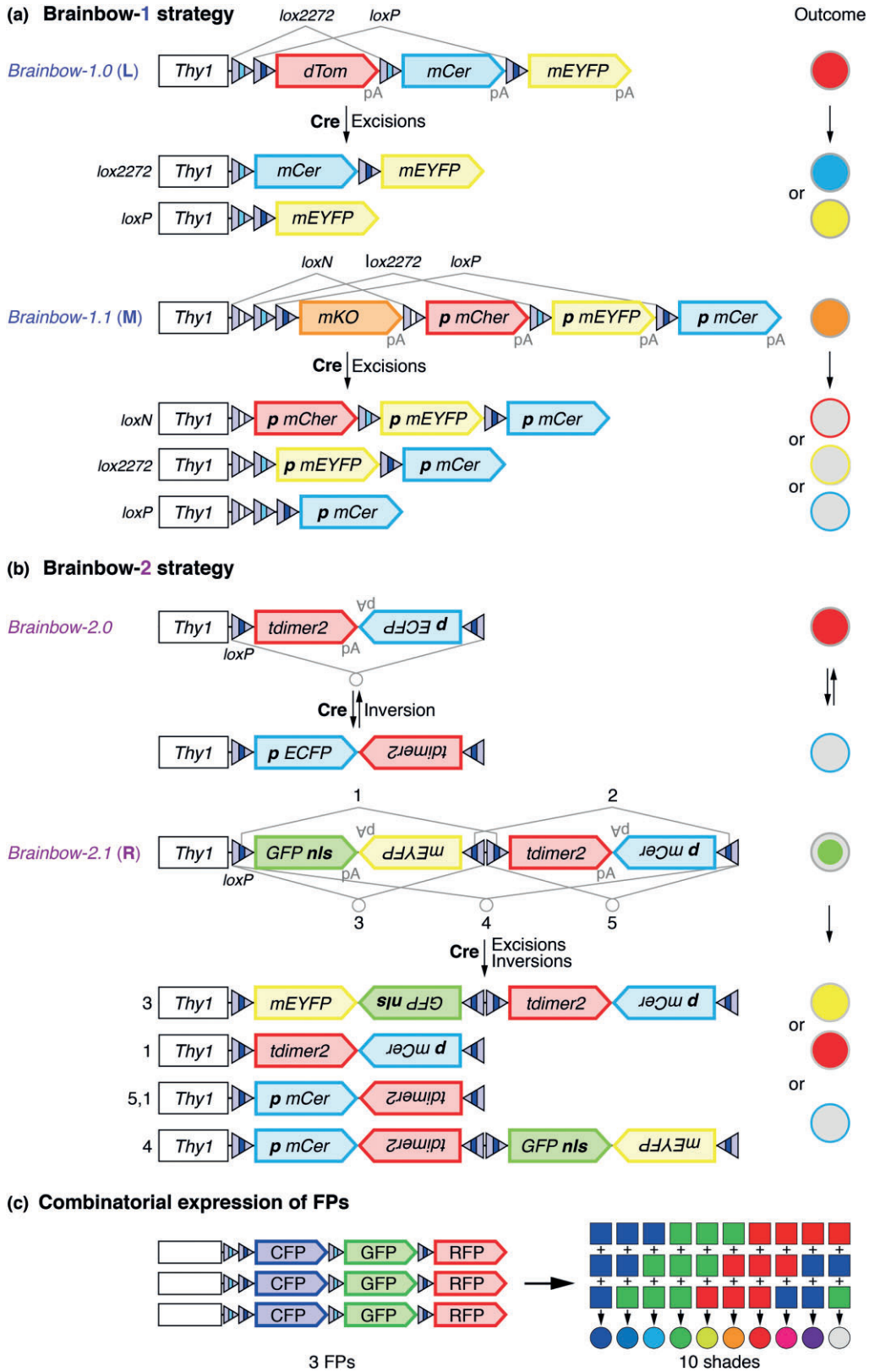


FIGURE 2 | Legend on next page.

of inducible Cre transgenes (e.g., CreER and the more sensitive variant CreERT2), in which the recombinase has been fused to a modified ligand-binding domain of the human estrogen receptor.⁸⁷ This receptor is insensitive to endogenous estrogens but can be activated by a synthetic ligand, 4-OH tamoxifen. Cre is retained in the cytosol, and becomes functional after binding of tamoxifen and localization to the nucleus.⁸⁷ For approaches that rely on irreversible excisions, spatiotemporal control of Cre or inducible Cre can also be achieved by tissue-specific enhancer fragments.⁸⁷ To achieve tissue or cell-type specificity, *Drosophila* multicolor labeling techniques tend to control the expression of Brainbow transgenes, whereas tools designed for mice frequently restrict recombinase expression.

ASSEMBLY INTO GENETIC MULTICOLOR LABELING TOOLS

Brainbow Blueprints

Exploiting the expanding FP color palette and site-specific recombination technologies, multicolor labeling was first achieved by the Brainbow system devised by Livet et al. for mice.² This creative approach takes advantage of the Cre-*lox* system to stochastically drive the expression of one of three or four FPs from a single transgene in genetically defined cell populations. Brainbow transgenes follow two principles. The Brainbow-1 strategy relies on Cre-mediated excision of DNA fragments using heterospecific *lox* sites (Figure 2(a)). In *Brainbow-1.0* and *-1.1* transgenes, three *lox* pairs (*loxN*, *lox2272*, and *loxP*) are astutely positioned in the same orientation adjacent to three or four linearly arranged FP-encoding cDNAs. These are each followed by *polyA* termination sequences to prevent transcriptional read-through. The FP located closest to the promoter is expressed by default. Upon Cre activation, site-specific recombination between identical *lox* pairs causes the excision of one, two, or three FP sequences. Consequently, new FPs are randomly positioned closest to the promoter. This leads to

the stable, mutually exclusive expression of one of three or four FPs per cell in a tissue. By contrast, the Brainbow-2 strategy makes use of inversion and excision events between a single type of recombination site, *loxP* (Figure 2(b)). The coding sequences of two FPs are arranged in opposite orientations in an invertible cassette flanked by inward-facing *loxP* sites. *Brainbow-2.0* contains one such cassette, and Cre-mediated inversion results in the differential expression of two markers. *Brainbow-2.1* transgenes consist of two adjacent cassettes. Recombination of *loxP* pairs in opposite or identical orientation leads to inversion and excision of cassettes, respectively. This results in four color-outcomes. Because inversions are reversible, transient Cre expression is required. Brainbow transgenes are controlled by the *Thy-1* enhancer to activate expression in neurons or glia, while recombination events are mediated by ubiquitous or tissue-specific Cre transgenes.

Color diversity can be in principle increased by adding more FPs with different emission spectra or epitope-tags to the constructs. However, this strategy is limited by the spectral emission signals of available FPs that confocal microscope detectors can realistically separate with sufficient brightness. Brainbow transgenes therefore use an alternative approach, the combinatorial expression of three or four FPs in two or more copies to increase the number of hues in a sample² (Figure 2(c)). Tandem integration of constructs into the mouse genome after injection into oocytes allows independent combinatorial expression of markers from multiple transgene copies. Depending on the number of transgenes present, cells can be labeled in >100 hues and individually traced by distinct color profiles using sophisticated image processing and analysis software.

Adjustments for Use in Flies, Zebrafish, Mice, and Chicken

The two original Brainbow strategies served as blueprints for the subsequent development of multicolor labeling technologies in *Drosophila* and

FIGURE 2 | Principles of mouse Brainbow blueprints. (a) Brainbow-1 strategy transgenes (blue) build on the ability of Cre to mediate excisions between heterospecific *lox* pairs orientated in the same direction. In *Brainbow-1.0* (L), dTomato (dTom) is expressed by default. Cre catalyzes recombination events between *lox2272* or *loxP* pairs, resulting in the stochastic expression of mCerulean (mCer) or mEYFP, respectively. In *Brainbow-1.1* (M), the default marker is mKusabira Orange (mKO). Cre mediates recombination between *loxN*, *lox2272*, and *loxP* pairs, allowing the expression of mCherry (mCher), mEYFP or mCerulean. A palmitoylation signal (*p*) targets these FPs to the membrane. *pA*, polyadenylation signals. (b) Brainbow-2 strategy transgenes (purple) use the ability of Cre to mediate inversions and excisions between *loxP* sites oriented in the opposite and the same direction, respectively. *Brainbow-2.0* consists of one invertible cassette. tdimer2 is expressed by default. Cre triggers reversible inversions between *loxP* sites, inducing expression of palmitoylated ECFP. *Brainbow-2.1* (R) consists of two invertible cassettes. Nuclear (nls) GFP is expressed by default. Cre-mediated inversions and excisions between *loxP* pairs allow expression of mEYFP, tdimer2 or palmitoylated mCerulean. All transgenes are under the control of the nervous system specific *Thy1* enhancer. (c) Combinatorial expression of blue, green, and red FPs from three transgene copies increases the color palette from 3 to 10 hues. References for transgenes are provided in Table 1.

Drosophila

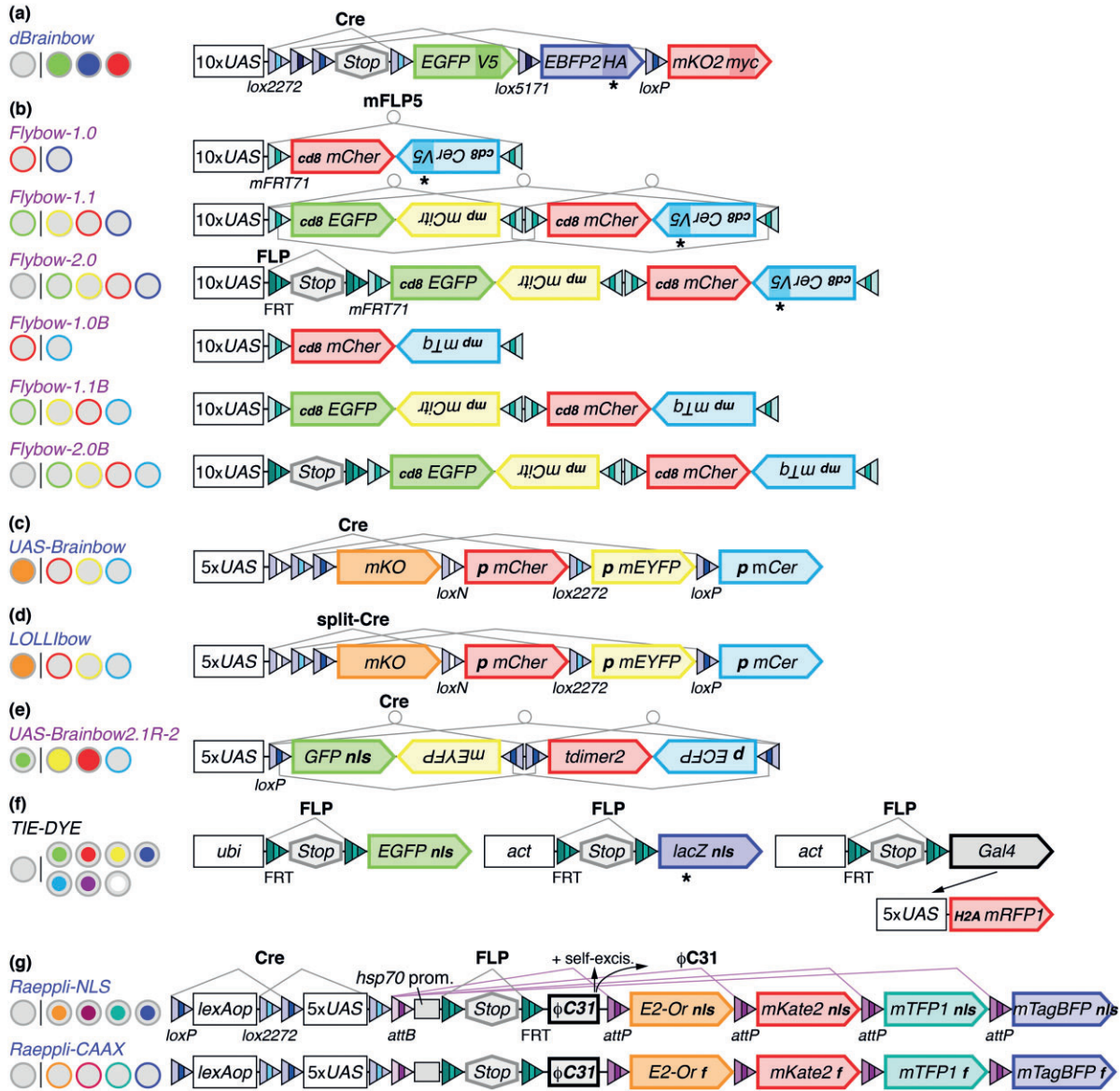
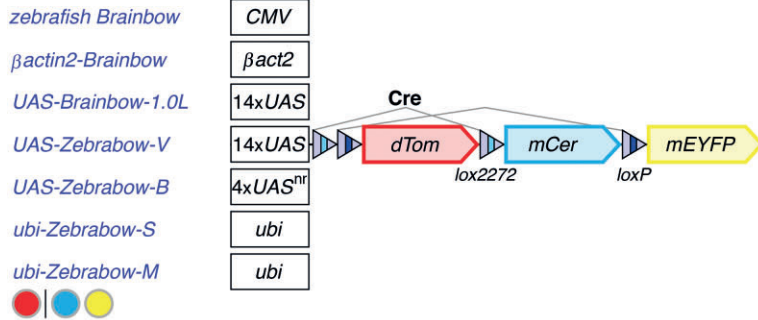
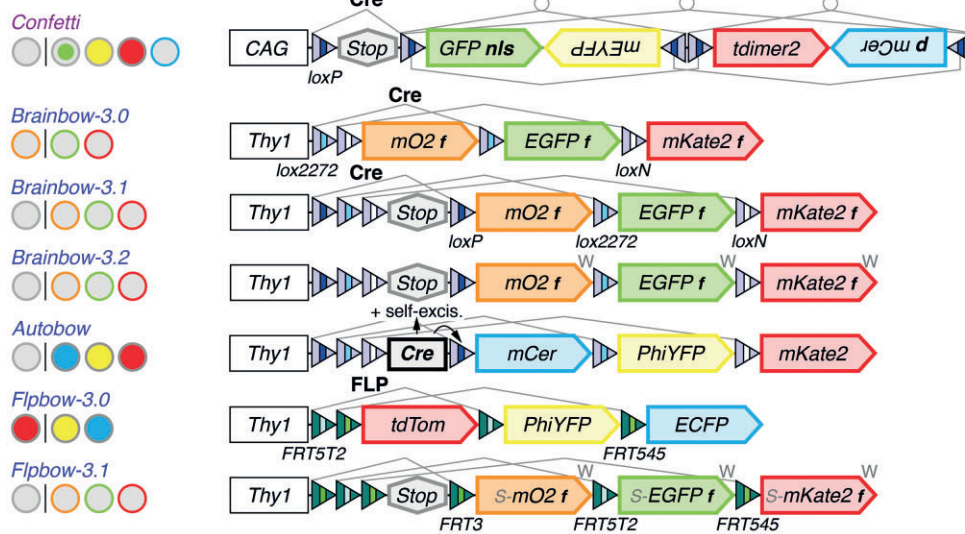


FIGURE 3 | Multicolor labeling tools in *Drosophila*. Transgenes following the excision-based Brainbow-1 strategy are highlighted in blue. Transgenes modeled on the inversion/excision-based Brainbow-2 strategy are shown in purple. Constructs are downstream of upstream activation sequences (UAS). (a) In *dBrainbow*, a stop cassette prevents marker expression prior to Cre activation. FPs are detected with three epitope-tags. Native fluorescence signals can be collected for EGFP and mKusabira Orange2 (mKO2); EBFP2 requires detection by immunolabeling (asterisk). (b) In *Flybow*, FPs are membrane-tethered using cd8 or myristoylation-palmitoylation (mp) sequences. *Flybow B* transgenes use mTurquoise (mTq) instead of V5-tagged mCerulean (mCer), which requires immunodetection (asterisk). *Flybow-1.0*, *1.1*, *1.0B*, and *1.1B* transgenes show default expression of mCherry (mCher) or EGFP. *Flybow-2.0* and *2.0B* require FLP-mediated excision of a FRT-site flanked stop cassette. Recombination events between *mFRT71* sites are triggered by mFLP5. (c-e) *UAS-Brainbow*, *LOLLiB*, and *UAS-Brainbow2.1R-2*, are derived from the mouse Brainbow transgenes M and R. Recombination events are mediated by Cre. *LOLLiB* relies on photo-activated split-Cre. p, palmitoylation signal. (f) In *TIE-DYE*, FLP mediates the excision of stop cassettes in three separate transgenes controlled by *ubiquitin* (*ubi*) or *actin* (*act*) enhancers. Gal4 leads to expression of mRFP1. *lacZ* requires detection with an antibody against β Gal (asterisk). Seven color outcomes are possible for the combination of these markers, targeted by a nuclear localization signal (nls) or Histone-2A (H2A). (g) *Raeppli* transgenes are downstream of *lexAop* or *UAS*. Cre-mediated excision converts transgenes into exclusively Gal4 or LexA controlled constructs. FLP-mediated excision of a FRT-flanked stop cassette, enables ϕ C31 transcription. Integrase expression is controlled by the full heat shock protein 70 (*hsp70*) promoter or *UAS*. This leads to recombination between the *attB* site and one of the four *attP* sites preceding each FP and to integrase self-excision. E2-Or, E2-Orange. FPs label cell nuclei in *Raeppli-NLS*, and cell membranes using a farnesylation (f) signal in *Raeppli-CAAX*. References for transgenes are provided in Table 1.

(a) Zebrafish



(b) Mouse



(c) Electroporation in chick and mice

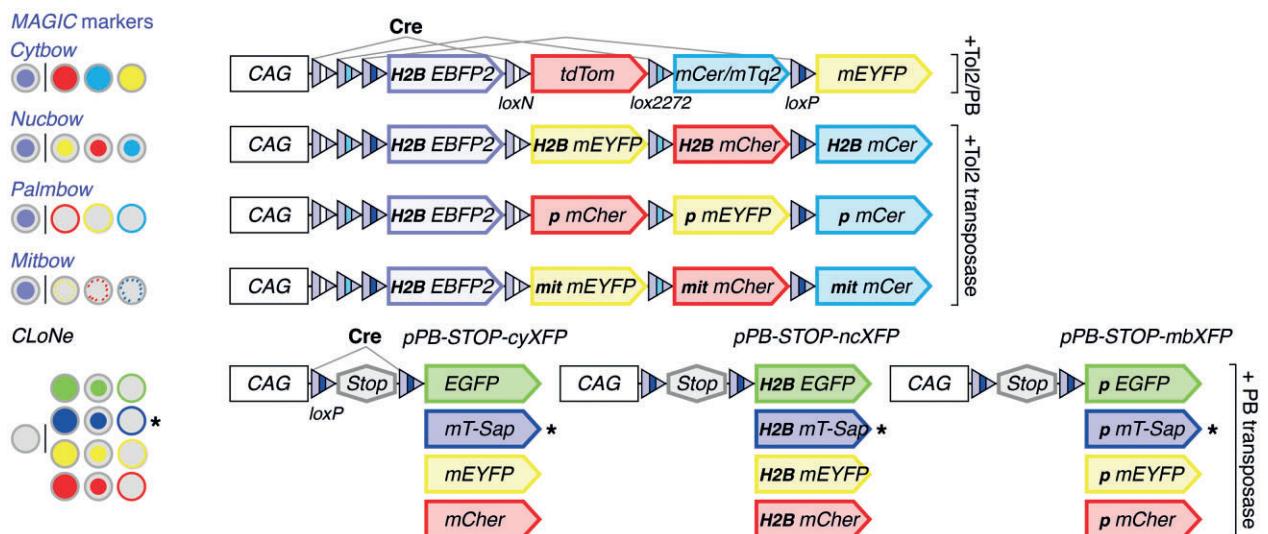


FIGURE 4 | Legend on next page.

vertebrate model organisms. Adjustments include specific adaptations for each animal species, as well as optimizations to overcome initial drawbacks and to increase the versatility of approaches.

Drosophila Multicolor Cell Labeling Approaches

Naturally, because of their alluring genetics, Brainbow technologies found their way into the toolbox of Drosophilists. *dBrainbow*³ and *Flybow*⁴ transgenes made a start on adapting the original strategies for use in flies. To take advantage of the increasing number of available Gal4 lines for controlling expression in any genetically accessible cell subpopulation and tissue of interest, both methods rely on *UAS* activated transcription. To boost the expression levels of reporter genes, constructs use 10 instead of 5 *UAS* repeats. Moreover, to avoid position effects, constructs are inserted into the genome by ϕ C31-mediated integration into genomic *attP* landing sites that show a high level of expression in the presence of Gal4 and no residual expression in its absence.

*dBrainbow*³ is modeled on the Brainbow-1 strategy and uses Cre-mediated recombination of heterospecific *lox* sites (Figure 3(a)). A transcriptional stop cassette precedes the series of three FP-encoding sequences to ensure that cells are solely labeled upon Cre expression. Moreover, each FP is tagged with a different epitope (V5, HA, and myc), which can be detected by immunohistochemistry. This helps to boost labeling intensities when endogenous fluorescence signals are inherently low or quenched during fixation of tissues. By contrast, *Flybow* transgenes⁴

are based on the Brainbow-2 strategy (Figure 3(b)). To bypass the limitations of Cre in flies, *Flybow* uses the *mFLP5-mFRT71* system⁷⁷ as an orthogonal tool that can be combined with the canonical *FLP-FRT* system. *mFLP5* is controlled by the heat-shock promoter. Transient exposure to heat induces the expression of *mFLP5*, which mediates inversions and excisions of cassettes flanked by *mFRT71* sites. Moreover, to facilitate complete labeling of neurites, all FPs are membrane-tethered.^{43,36} Similar to mouse *Brainbow-2.0* and *-2.1* transgenes, *Flybow-1.0* and *-1.1* constructs consist of one and two cassettes, respectively. In *Flybow-2.0*, an additional transcriptional stop cassette flanked by *FRT* sites in the same orientation precedes the invertible cassettes to eliminate default marker expression. The stop cassette is excised after induction of the canonical *FLP* recombinase. Transient *FLP* expression facilitates both sparse labeling and increases the color diversity because all four FPs can be used for tracing. Because *Flybow-2.0* relies on both *FLP* and *mFLP5*, it additionally can serve as an intersectional tool to refine expression, when *FLP* expression is controlled by a different cell-specific enhancer. The initial set of *Flybow* constructs uses an epitope-tagged cyan FP mCerulean variant,³¹ which requires immunodetection because of its weak native emission in flies. To bypass the need for immunolabeling and to enable live imaging of endogenous fluorescence signals in all four channels, in a second set of transgenes (*Flybow-1.0B*, *1.1B* and *2.0B*)⁵ *cd8*-tethered mCerulean-V5 was replaced by the brighter myr-palm anchored mTurquoise.³²

FIGURE 4 | Multicolor labeling tools for use in zebrafish and mouse, as well as for electroporation in mouse and chicken. Constructs following the Brainbow-1 strategy are indicated in blue and constructs based on the Brainbow-2 strategy in purple. (a) In zebrafish, the mouse *Brainbow-1.0L* cassette has been placed downstream of four regulatory elements: the *cytomegalovirus* enhancer (*CMV*), the *β actin2* (*β act2*) enhancer, upstream activation sequences (*UAS*), or the ubiquitin (*ubi*) enhancer. *UAS-Zebrabow-B* uses non-repetitive (nr) tandem *UAS* sites. V, variegated; B, broad; S, single; M, multiple. (b) In *Confetti*, a stop cassette precedes the two invertible cassettes of the original mouse *Brainbow-2.1 (R)* transgene. Expression is controlled by *CAG*, the chicken *β -actin promoter with cytomegalovirus* (*CAG*) enhancer. Grey lines only indicate a subset of possible recombination events. *Thy1*-controlled *Brainbow-3.0*, *3.1*, *3.2* transgenes use farnesylated (f) FPs – mOrange2 (mO2), EGFP, and mKate2. In *Brainbow-3.1* and *3.2*, a stop cassette prevents default FP expression. In *Brainbow-3.2*, a woodchuck hepatitis virus posttranscriptional regulatory element (*W*) has been placed downstream of each FP. In *Autobow*, *Thy1* controls expression of *lox*-flanked Cre to trigger recombination events and self-excision. In *Flybow-3.0* and *3.1* transgenes, *FLP* mediates recombination of spacer variant pairs *FRT3*, *FRT5T2*, and *FRT545*. *Flybow-3.1* uses a stop cassette and FP fused with a SUMOstar tag (S) for immunodetection. mCer, mCerulean; PhiYFP, Phialidium YFP; tdTom, tandem dimer Tomato. (c) *MAGIC* and *CLoNe* plasmids are transposon-based vectors suitable for electroporation experiments in mouse and chicken. Tol2 or PiggyBac (PB) transposases promote the genomic integration of vectors. Ubiquitous or tissue/cell-type specific Cre is provided by co-injected vectors (chick and mouse) or by expression from genomic insertions (mouse). FP expression is controlled by the *CAG* regulatory element. In *MAGIC* markers, four different FPs are expressed from single vectors. FP are localized in the cytoplasm (*Cytbow*), in nuclei using Histone-2B (H2B) fusions (*Nucbow*), in the membrane using a palmitoylation (p) signal (*Palmbow*) or in mitochondria (mit) using a targeting signal from human *COX8* (*Mitbow*). H2B-EBFP2 is expressed in unrecombined cells. In the *CLoNe* approach, four FPs [EGFP, mT-Sapphire (mT-Sap), mEYFP, and mCherry] are expressed from twelve separate labeling vectors. FPs are either cytoplasmic (cy), or nuclear (nc), and membrane-bound (mb) using H2B or palmitoylation tags, respectively. A stop cassette prevents default expression of markers in the absence of Cre. Stable multicolor labeling is achieved by different random combinations of vector insertions and expression in individual cells. Asterisk indicates that mT-Sapphire was assigned the color blue, although the maximum emission is in the green/yellow range. References for transgenes are provided in Table 1.

Three subsequent *Drosophila* multicolor cell labeling methods take advantage of original mouse *Brainbow-1* and *-2* constructs. In *UAS-Brainbow* (Figure 3(c))⁶ and *LOLLIbow* (live imaging optimized multicolor labeling by light-inducible *Brainbow*; Figure 3(d)),⁷ the mouse *Brainbow-1.1* (*M*) cassette was inserted into different *UAS* vectors. Similarly, in *UAS-Brainbow2.1R-2* (Figure 3(e)),⁸ the mouse *Brainbow-2.1* (*R*) fragment containing two invertible cassettes was transferred into a *UAS* vector. The constitutively-active *hsp70-Mos1-Cre* (Ref 80) and a new heat shock-inducible *hs-Cre-HA* line⁸ are used in conjunction with *UAS-Brainbow* and *UAS-Brainbow2.1R-2* transgenes, respectively. By contrast in *LOLLIbow*, recombination events are controlled by a photo-inducible split-Cre version.⁷ The N- and C-terminal fragments of Cre were fused with two plant proteins—a truncated version of CIB1 (CIBN) and nuclear targeted Cryptochrome 2 (CRY2)—and subcloned into *UAS* vectors. Gal4 activates the simultaneous expression of these chimeric proteins while brief exposure to blue light induces their dimerization to reconstitute a functional enzyme.

Two other additions to the toolkit, *TIE-DYE*⁹ and *Raepli*,¹⁰ have been designed to support whole-tissue multicolor labeling by increasing the recombination efficiency. Unlike the other approaches, *TIE-DYE* (three independent excisions dye) does not rely on a single but a combination of four separate, previously generated transgenes⁹ (Figure 3(f)). Upon heat shock, FLP induces the expression of nuclear GFP, β -Galactosidase or Gal4 by stochastically excising FLP-out stop cassettes that are positioned between the widely active enhancers *actin* or *ubiquitin* and the reporters. Gal4 in turn activates expression of nuclear RFP from a fourth *UAS* controlled transgene. When visualizing *lacZ* by immunolabeling with a secondary antibody coupled to a far-red fluorophore, clones can be labeled in up to seven hues, because combinations of several excision events can occur in each cell. Moreover, in conjunction with *UAS*-based knockdown or over-expression transgenes, effects of genetic manipulations on subsets of clones that co-express RFP can be compared with control clones that express GFP and/or β -Galactosidase but not RFP. *Raepli* (named after the Basel carnival confetti)¹⁰ makes use of all three recombination systems in a single versatile transgene (Figure 3(g)). Transgenes are under the dual control of *lexAop* and five *UAS* repeats, which are flanked by heterospecific *lox* pairs, leaving all options open for genetic manipulations by two independent binary systems. Moreover, Cre can be used to catalyze excision events that produce stable strains with restricted *UAS*

or *lexAop* controlled transgenes in the same genetic locus. Because insertions are influenced by their chromosomal positions, this trick ensures that expression levels remain identical, since no additional injections are required to generate separate lines. *Raepli* follows the *Brainbow-1* strategy to control the selection and expression of markers. However, instead of Cre or FLP, ϕ C31 catalyzes the excisions. One *attB* site follows the *lexAop* and *UAS* repeats, while *attP* recombination sites each precede the sequences of four linearly arranged FPs. These are either nuclear or targeted to the membrane by a farnesylation signal. Importantly, the transgenes include the ϕ C31 coding sequence, which has been placed downstream of a full *heat shock protein 70* (*hsp70*) promoter. A *FRT*-flanked stop cassette, positioned between the promoter and the integrase, reduces low-level background activity of ϕ C31 while providing means for temporal control. Heat- or Gal4-induced FLP leads to excision of the stop cassette. This enables ϕ C31 expression controlled by the activity of the heat shock promoter or *UAS*. The integrase in turn catalyzes the recombination between the *attB* and one of the four *attP* sites, resulting in the stable selection of one FP, as well as self-excision.

Unlike in mice, fly transgenes integrate as single copies into genomic loci. The number of *UAS*-controlled transgenes can be increased by standard genetic crosses. Doubling the transgenes with three or four FPs extends the number of detectable hues to 6 or 10.^{3,7,10} The addition of further copies in one animal is possible but genetic crosses become increasingly complex due to the limited set of chromosomes. Because *Drosophila* multicolor labeling tools use the Gal4-*UAS* system, they can readily be combined with *UAS*-based RNA interference or over-expression constructs for knockdown and gain-of-function approaches.^{93,94} Moreover, *Brainbow* tools that do not rely on canonical FLP-*FRT* site-specific recombination and involve a small number of transgenes, can also be combined with loss-of-function approaches such as mosaic analysis with a repressible cell marker (MARCM).⁶³

Adaptations in Zebrafish

Multicolor labeling approaches developed for zebrafish utilize the mouse *Brainbow-1.0* (*L*) cassette (Figure 4(a)). In zebrafish *Brainbow*, this cassette is positioned downstream of the *cytomegalovirus* (CMV) promoter in a commonly used expression vector, that allows transient ubiquitous expression after injection.¹¹ *β actin2-Brainbow* goes one step further by using an *actin* enhancer in a stable transgenic line.¹² In *UAS-Brainbow-1.0L*,¹³ and *ZebraBow*,¹⁴

tissue-specific transgene expression is controlled either by 14 *UAS* repeats (*UAS-Brainbow1.0L* with at least 3 insertions and *UAS-Zebrabow-V* with 2 insertions) or four non-repetitive *UAS* sequences (*UAS-Zebrabow-B* with 9–31 copies). In the presence of Gal4, the former results in variegated mosaic expression because repeat sequences are prone to CpG methylation and randomly silenced,⁹⁵ thus rendering this strategy highly suitable for sparse labeling. By contrast, tandem *UAS* sites with four unique sequences are less susceptible to methylation, thus enabling broad cell labeling. Additional Zebrabow transgenes are controlled by the *ubiquitin* enhancer and either contain a single (*ubi-Zebrabow-S*) or multiple (16–32) insertions (*ubi-Zebrabow-M*).¹⁴ While transgenic lines with a high number of insertions in principle produce many hues, data analysis may be limited by the capacity of image processing software in achieving the necessary resolution of colors. Site-specific recombination events are mediated by Cre, which can be delivered by microinjection of a purified protein. Alternatively, zebrafish transgenics can be crossed with heat shock-inducible Cre or tamoxifen-inducible CreER lines that either are widely expressed or controlled by tissue-specific enhancers.¹⁴

Second and Third Generations of Mouse Brainbow Transgenes

The expression of a default FP in the first generation of mouse Brainbow strategies represents a potential limitation for some applications. Therefore, in Confetti mice,¹⁵ a *loxP* flanked stop cassette was added upstream of the two invertible cassettes in the *Brainbow-2.1 (R)* transgene. Similar to *dBrainbow*³ and *Flybow 2.0*,⁴ this ensures that cells express FPs only after recombinase-mediated excision of this cassette.

Six years after their first publication,² mouse Brainbow transgenes underwent a redesign.¹⁶ *Brainbow-3.0* transgenes switched to different FPs, mOrange2, EGFP and mKate2, because they are spectrally and antigenically distinct, show less tendency to aggregate and are highly stable upon illumination and after fixation. To evenly label axons and dendrites, the FPs were membrane-tethered using a farnesylation sequence. In *Brainbow-3.1*, a non-fluorescing mutated YFP from the hydrozoan *Phialidium* (PhiYFP) occupies the default position to function as a stop cassette. Importantly, mutated YFP can still be detected by antibody labeling to visualize cells that have not undergone recombination. In *Brainbow-3.2*, a woodchuck hepatitis virus post-transcriptional regulatory element (WPRE) was inserted downstream of each FP sequence to increase protein levels. To reduce the number of

required crosses, similar to *Raepli*, in *Autobow* transgenes a stop cassette containing Cre recombinase cDNA was placed upstream of the linearly arranged FP sequences. When neurons begin to differentiate, the *Thy1* regulatory element leads to expression of Cre. The enzyme subsequently catalyzes recombination events that allow both the expression of FPs and self-excision. While lacking temporal and spatial control, this approach helps to accelerate the analysis of loss-of-function phenotypes because only one transgene needs to be combined with mutant alleles. Finally to serve as orthogonal labeling systems, in two *Flpbow* transgenes, *lox* sites were replaced by incompatible *FRT* spacer variants (*FRT3*, *FRT5T2*, and *FRT545*) to allow FLP-mediated recombination events.

Vectors for Embryonic Electroporation in Mouse and Chicken

In mice and chicken, *in utero* and *in ovo* electroporation constitutes a widely used alternative technique to study nervous system development. Injection of plasmids into the brain ventricles, the central canal of the spinal cord or the optic vesicle, and application of an electric current make it possible to perform region-specific transfections of cells during restricted developmental time windows. Although targeted delivery of viral vectors can provide spatial and temporal control,^{16,96} applications are limited to neuroanatomical studies. Four recently developed sets of labeling vectors take advantage of the stochastic nature of plasmid integration following electroporation to enable multicolor lineage tracing. To ensure that labels are stably inherited during mitotic divisions, transposon-based vectors are co-electroporated with transposase-expressing plasmids to catalyze genomic integration. Two approaches, *PB IUP* (PiggyBac in utero electroporation)⁹⁷ and *Star Track*,⁹⁸ function independently of Cre and involve the electroporation of mixtures of separate plasmids, each driving expression of a single FP under the control of broadly active or cell-type specific enhancers. In *Star Track*, FPs are either cytoplasmic or targeted to the nucleus. The versatility of these methods is further extended by two additional Cre-dependent toolkits—*MAGIC* (multiaddressable genome-integrative color) markers¹⁷ and *CLoNe* (clonal labeling of neural progeny).¹⁸ These enable expression in neural precursors and their offspring, because vectors are under the control of the ubiquitous CAG promoter (Figure 4(c)). *MAGIC* and *CLoNe* vectors rely on random genomic integration of a small number of transposon-based vectors (one to three transposons per cell in the case of *MAGIC* markers). Co-injected plasmids in mouse or chick, or stably

inserted transgenes in mouse strains serve as sources for Cre. This provides an additional level of spatiotemporal control and specificity because the expression of Cre can be regulated by different enhancer elements. *MAGIC* constructs are based on the Brainbow-1 blueprint, in which stochastic expression of four FPs is obtained by Cre-mediated recombination events in a single vector. The first FP, nuclear EBFP, is expressed by default and followed by tdTomato or mCherry, mCerulean or mTurquoise2 and mEYFP arranged in varying order. In these vectors, FPs are either located in the cytoplasm (*Cytbow*) or targeted to nuclei (*Nucbow*), membranes (*Palmbow*) or mitochondria (*Mitbow*). By contrast, *CLoNe* vectors follow a similar principle as *Drosophila TIE-DYE*, *Star Track* or *PB-IUP*. Random expression of cytoplasmic, nuclear or membrane-bound FPs (EGFP, mT-Sapphire, mEYFP, and mCherry) is achieved by twelve separate vectors. A *loxP*-flanked stop cassette upstream of each FP prevents default expression in the absence of Cre. Importantly, in *Star Track*, *MAGIC* and *CLoNe* approaches, the co-electroporation of vectors with separable subcellular addresses facilitates the identification of clonally related cells by increasing the number of unique marker combinations—e.g., color and marker localization.

CONCLUSIONS

Brainbow technologies are a fascinating habitat for geneticists. The designs in different model organisms clearly inspired each other. The recent progress in molecular cloning techniques facilitated the assembly of genetic building blocks into sophisticated constructs. Moreover, steady technical advances in confocal and multiphoton microscopy made it possible to image differentially labeled cells with increasing ease. Some of the multicolor labeling tools have found their first successful applications in developmental studies in a number of tissues (Box 1) and more will undoubtedly follow. In parallel, new Brainbow methods are still in the making. What features would benefit most urgently from enhancements? Expression constructs generally seem to function well and are suitable for many applications. However, one drawback is still the control over recombination events, which requires most of the adjustments in each experimental situation. Recombination can occur in precursors or postmitotic progeny, independently of cell divisions. For morphological studies, as long as a subset of several cells in a sample has been labeled in different colors and unambiguous tracing is possible, it does not matter whether recombination happens in precursors or their offspring. By contrast, for lineage studies, it is crucial to trigger single recombination

BOX 1

BRAINBOW TECHNOLOGIES AT WORK

Brainbow methods were designed for anatomical and functional studies of genetically accessible cell populations with two main experimental applications in mind: (1) sparse labeling of specific cell types to visualize their morphologies and (2) comprehensive labeling of clonally related cells to track lineages (Figure 5). Consistently, Brainbow transgenes were so far successfully utilized to map known and new neuron subtypes,^{8,99} to identify the role of a basic helix-loop-helix transcription factor in axonal projection pattern formation,¹⁰⁰ and to monitor laminar map assembly¹³ in the visual systems of flies and zebrafish. Furthermore, visualization of single cell shapes in their epithelial environment provided insights into the role of the tyrosine kinase Src42A in embryonic tracheal tube elongation.⁶ In lineage tracing experiments, Brainbow technologies were employed to follow the development of individual embryonic peripheral glial cell subtypes into perineurial, subperineurial, and wrapping glial subtypes associated with third instar larval peripheral nerves in *Drosophila*.¹⁰¹ Finally, multicolor clonal analysis discovered the contributions of dominant cardiomyocyte lineages to zebrafish heart morphogenesis,¹² the role of neutral competition between symmetrically dividing intestinal crypt stem cells¹⁵ and the origin of stem cells required for corneal epithelial renewal in mice.¹⁰²

events specifically in precursors. In both situations, considering the small number of possible resolvable labels, a highly diverse color outcome is desired: in progeny, as this helps to increase the density of sparse labeling and thus the reconstruction of individual cells, and in precursors to follow many different lineages in parallel. Therefore means need to be found, by which high expression levels of recombinases can be induced transiently, with little delay and at a precise developmental stage. Moreover, recombinase variants could be designed, that are highly efficient at low levels, do not display any background activity and therefore require only brief enhancer activity to induce expression. Finally, similar to the light-inducible *split-Cre* strategy,⁷ inactive recombinase variants could be expressed at high levels from the outset, which are rapidly converted into active variants in response to an external signal applicable in all model organisms.

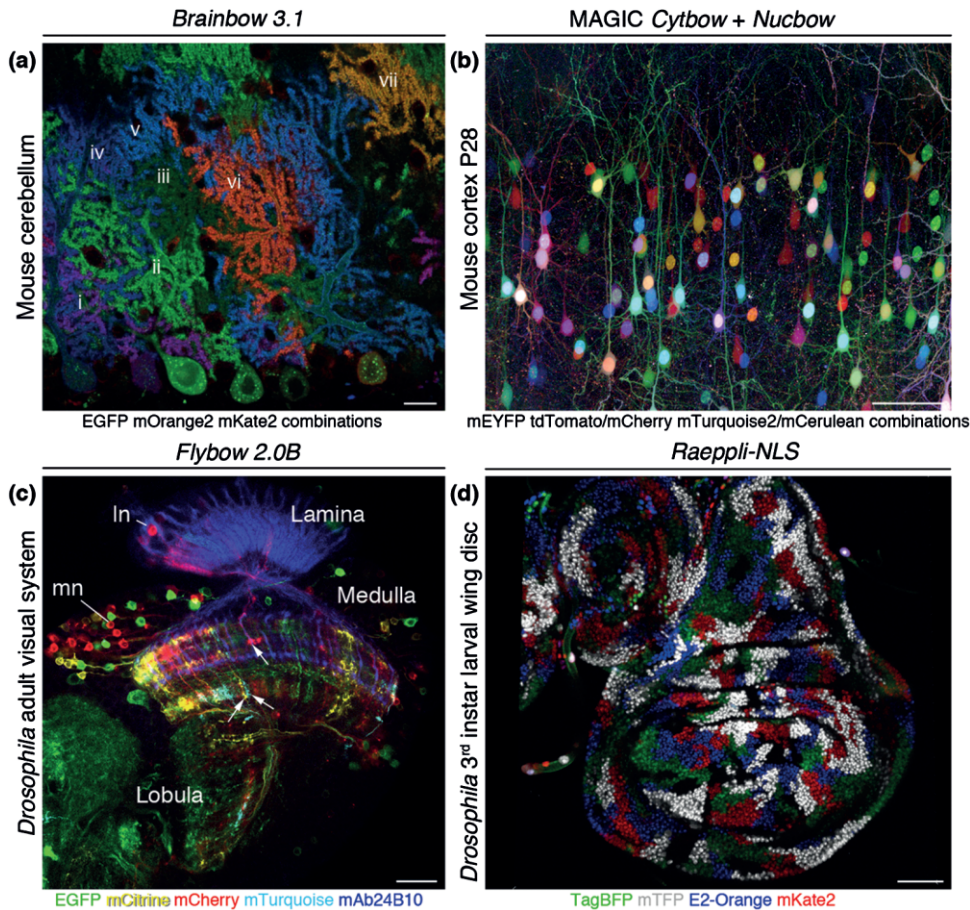


FIGURE 5 | Four examples of Brainbow technologies at work. (a) Purkinje cells in the mouse cerebellum are visualized in seven colors (i–vii) using *Brainbow-3.1* and *L7-Cre* transgenes, as well as antibody amplification. (Reprinted with permission from Ref 16. Copyright 2013 Nature Publishing Group) Scale bar, 20 μm . (b) Pyramidal neurons in the P28 cortex of a *CAG-CreERTM* mouse are labeled by combinations of co-electroporated *MAGIC Cytbow* and *Nucbow* markers at E15. The image was acquired by two-photon microscopy. (Reprinted with permission from Ref 17. Copyright 2014 Elsevier Ltd.) Scale bar, 100 μm . (c) Neurites of lamina and medulla neuron subtypes (ln, mn) in the adult *Drosophila* optic lobe are visualized by endogenous fluorescent protein signals using a *Flybow-2.0B* transgene, activated by *hs-mFLP5* and *NP4151-Gal4*—an enhancer trap insertion into the *Netrin B* locus. The image represents a single optical section. Several neurons (arrowheads) are suitable for tracing in stacks. Photoreceptor axons are visualized by immunolabeling with mAb24B10 (blue). Scale bar, 20 μm . (d) Nuclei of epithelial cell clones in a 3rd instar larval wing disc of *Drosophila* are labeled by four fluorescent proteins using a *Raepli-NLS* transgene, activated by *tubulin-Gal4* and *UAS-FLP*. This approach facilitates the comprehensive analysis of clones in the entire tissue. (Reprinted with permission from Ref 10. Copyright 2014 The Company of Biologists Ltd.) Scale bar, 50 μm .

Parallel efforts could be dedicated to further extend the functionality of Brainbow approaches by connecting one color outcome with an additional subcellular marker, such as a presynaptic protein, or a specific genetic manipulation. This is to some extent possible with the TIE-DYE approach.⁹ To reduce the number of required transgenes and complexity of genetic crosses, the self-processing 2A peptide sequence¹⁰³ represents a valuable alternative, as it can be placed between two proteins to achieve co-translational cleavage and bicistronic expression. Loulier et al. showed that a dominant-negative

form of one molecular determinant and one FP can be co-expressed with the 2A system to report genetic mosaic perturbations in mice.¹⁷ Similarly in *Drosophila*, LexA, or QF could be linked to one FP and used in conjunction with *lexAop* or *QUAS*-based knockdown or over-expression transgenes to study the effects of a genetic manipulation on a subset of clones. These possibilities underscore that multicolor cell labeling tools are here to stay and will evolve further. They will continue to unlock doors and provide us with access to our cells of choice, making them visible in bright colors with the strokes of genetic paintbrushes.

ACKNOWLEDGMENTS

We apologize to colleagues, whose work was not included in this review because of our focus on inheritable recombinase-based multicolor labeling tools in vertebrate and invertebrate model organisms. We are grateful to D. Cai and J. Sanes, E. Beaurepaire and J. Livet, O. Kanca and M. Affolter for providing the images shown in Figure 5. We thank A.S. Chiang for the information on *hs-Cre-HA*, and H. Apitz, R. Kaschula and N. Shimosako for helpful comments on the manuscript. Research in our laboratory is funded by the Medical Research Council (U117581332).

REFERENCES

- Lee T. Generating mosaics for lineage analysis in flies. *WIREs Dev Biol* 2014, 3:69–81.
- Livet J, Weissman TA, Kang H, Draft RW, Lu J, Bennis RA, Sanes JR, Lichtman JW. Transgenic strategies for combinatorial expression of fluorescent proteins in the nervous system. *Nature* 2007, 450:56–62.
- Hampel S, Chung P, McKellar CE, Hall D, Looger LL, Simpson JH. Drosophila Brainbow: a recombinase-based fluorescence labeling technique to subdivide neural expression patterns. *Nat Methods* 2011, 8:253–259.
- Hadjiconomou D, Rotkopf S, Alexandre C, Bell DM, Dickson BJ, Salecker I. Flybow: genetic multicolor cell labeling for neural circuit analysis in *Drosophila melanogaster*. *Nat Methods* 2011, 8:260–266.
- Shimosako N, Hadjiconomou D, Salecker I. Flybow to dissect circuit assembly in the *Drosophila* brain. *Methods Mol Biol* 2014, 1082:57–69.
- Forster D, Luschnig S. Src42A-dependent polarized cell shape changes mediate epithelial tube elongation in *Drosophila*. *Nat Cell Biol* 2012, 14:526–534.
- Bouline M, Samarajeewa H, Baker JD, Kim MD, Chiba A. Live imaging of multicolor-labeled cells in *Drosophila*. *Development* 2013, 140:1605–1613.
- Chin AL, Lin CY, Fu TF, Dickson BJ, Chiang AS. Diversity and wiring variability of visual local neurons in the *Drosophila* medulla M6 stratum. *J Comp Neurol* 2014, 522:3795–3816.
- Worley MI, Setiawan L, Hariharan IK. TIE-DYE: a combinatorial marking system to visualize and genetically manipulate clones during development in *Drosophila melanogaster*. *Development* 2013, 140:3275–3284.
- Kanca O, Caussinus E, Denes AS, Percival-Smith A, Affolter M. Raeppli: a whole-tissue labeling tool for live imaging of *Drosophila* development. *Development* 2014, 141:472–480.
- Pan YA, Livet J, Sanes JR, Lichtman JW, Schier AF. Multicolor Brainbow imaging in zebrafish. *Cold Spring Harb Protoc* 2011, 2011:prot5546.
- Gupta V, Poss KD. Clonally dominant cardiomyocytes direct heart morphogenesis. *Nature* 2012, 484:479–484.
- Robles E, Filosa A, Baier H. Precise lamination of retinal axons generates multiple parallel input pathways in the tectum. *J Neurosci* 2013, 33:5027–5039.
- Pan YA, Freundlich T, Weissman TA, Schoppik D, Wang XC, Zimmerman S, Ciruna B, Sanes JR, Lichtman JW, Schier AF. Zebrafish: multispectral cell labeling for cell tracing and lineage analysis in zebrafish. *Development* 2013, 140:2835–2846.
- Snippert HJ, van der Flier LG, Sato T, van Es JH, van den Born M, Kroon-Veenboer C, Barker N, Klein AM, van Rheenen J, Simons BD, et al. Intestinal crypt homeostasis results from neutral competition between symmetrically dividing Lgr5 stem cells. *Cell* 2010, 143:134–144.
- Cai D, Cohen KB, Luo T, Lichtman JW, Sanes JR. Improved tools for the Brainbow toolbox. *Nat Methods* 2013, 10:540–547.
- Loulier K, Barry R, Mahou P, Le Franc Y, Supatto W, Matho KS, Ieng S, Fouquet S, Dupin E, Benosman R, et al. Multiplex cell and lineage tracking with combinatorial labels. *Neuron* 2014, 81:505–520.
- Garcia-Moreno F, Vasistha NA, Begbie J, Molnar Z. CLoNe is a new method to target single progenitors and study their progeny in mouse and chick. *Development* 2014, 141:1589–1598.
- Shimomura O, Johnson FH, Saiga Y. Extraction, purification and properties of aequorin, a bioluminescent protein from the luminous hydromedusa, *Aequorea*. *J Cell Comp Physiol* 1962, 59:223–239.
- Chalfie M, Tu Y, Euskirchen G, Ward WW, Prasher DC. Green fluorescent protein as a marker for gene expression. *Science* 1994, 263:802–805.
- Shagin DA, Barsova EV, Yanushevich YG, Fradkov AF, Lukyanov KA, Labas YA, Semenova TN, Ugalde JA, Meyers A, Nunez JM, et al. GFP-like proteins as ubiquitous metazoan superfamily: evolution of functional features and structural complexity. *Mol Biol Evol* 2004, 21:841–850.
- Ai HW, Henderson JN, Remington SJ, Campbell RE. Directed evolution of a monomeric, bright and photostable version of *Clavularia* cyan fluorescent protein: structural characterization and applications in fluorescence imaging. *Biochem J* 2006, 400:531–540.
- Matz MV, Fradkov AF, Labas YA, Savitsky AP, Zaraisky AG, Markelov ML, Lukyanov SA.

- Fluorescent proteins from nonbioluminescent Anthozoa species. *Nat Biotechnol* 1999, 17:969–973.
24. Karasawa S, Araki T, Nagai T, Mizuno H, Miyawaki A. Cyan-emitting and orange-emitting fluorescent proteins as a donor/acceptor pair for fluorescence resonance energy transfer. *Biochem J* 2004, 381:307–312.
 25. Sakaue-Sawano A, Kurokawa H, Morimura T, Hanyu A, Hama H, Osawa H, Kashiwagi S, Fukami K, Miyata T, Miyoshi H, et al. Visualizing spatiotemporal dynamics of multicellular cell-cycle progression. *Cell* 2008, 132:487–498.
 26. Shcherbo D, Murphy CS, Ermakova GV, Solovieva EA, Chepurnykh TV, Shcheglov AS, Verkhusha VV, Pletnev VZ, Hazelwood KL, Roche PM, et al. Far-red fluorescent tags for protein imaging in living tissues. *Biochem J* 2009, 418:567–574.
 27. Ai HW, Shaner NC, Cheng Z, Tsien RY, Campbell RE. Exploration of new chromophore structures leads to the identification of improved blue fluorescent proteins. *Biochemistry (Mosc)* 2007, 46:5904–5910.
 28. Subach OM, Gundorov IS, Yoshimura M, Subach FV, Zhang J, Gruenwald D, Souslova EA, Chudakov DM, Verkhusha VV. Conversion of red fluorescent protein into a bright blue probe. *Chem Biol* 2008, 15:1116–1124.
 29. Tsien RY. The green fluorescent protein. *Annu Rev Biochem* 1998, 67:509–544.
 30. Miyawaki A, Tsien RY. Monitoring protein conformations and interactions by fluorescence resonance energy transfer between mutants of green fluorescent protein. *Methods Enzymol* 2000, 327:472–500.
 31. Rizzo MA, Springer GH, Granada B, Piston DW. An improved cyan fluorescent protein variant useful for FRET. *Nat Biotechnol* 2004, 22:445–449.
 32. Goedhart J, van Weeren L, Hink MA, Vischer NO, Jalink K, Gadella TW Jr. Bright cyan fluorescent protein variants identified by fluorescence lifetime screening. *Nat Methods* 2010, 7:137–139.
 33. Goedhart J, von Stetten D, Noirclerc-Savoie M, Lelimosin M, Joosen L, Hink MA, van Weeren L, Gadella TW Jr, Royant A. Structure-guided evolution of cyan fluorescent proteins towards a quantum yield of 93%. *Nat Commun* 2012, 3:751.
 34. Zapata-Hommer O, Griesbeck O. Efficiently folding and circularly permuted variants of the Sapphire mutant of GFP. *BMC Biotechnol* 2003, 3:5.
 35. Ai HW, Hazelwood KL, Davidson MW, Campbell RE. Fluorescent protein FRET pairs for ratiometric imaging of dual biosensors. *Nat Methods* 2008, 5:401–403.
 36. Zacharias DA, Violin JD, Newton AC, Tsien RY. Partitioning of lipid-modified monomeric GFPs into membrane microdomains of live cells. *Science* 2002, 296:913–916.
 37. Griesbeck O, Baird GS, Campbell RE, Zacharias DA, Tsien RY. Reducing the environmental sensitivity of yellow fluorescent protein. Mechanism and applications. *J Biol Chem* 2001, 276:29188–29194.
 38. Strack RL, Bhattacharyya D, Glick BS, Keenan RJ. Noncytotoxic orange and red/green derivatives of DsRed-Express2 for whole-cell labeling. *BMC Biotechnol* 2009, 9:32.
 39. Shaner NC, Lin MZ, McKeown MR, Steinbach PA, Hazelwood KL, Davidson MW, Tsien RY. Improving the photostability of bright monomeric orange and red fluorescent proteins. *Nat Methods* 2008, 5:545–551.
 40. Campbell RE, Tour O, Palmer AE, Steinbach PA, Baird GS, Zacharias DA, Tsien RY. A monomeric red fluorescent protein. *Proc Natl Acad Sci USA* 2002, 99:7877–7882.
 41. Shaner NC, Campbell RE, Steinbach PA, Giepmans BN, Palmer AE, Tsien RY. Improved monomeric red, orange and yellow fluorescent proteins derived from *Discosoma* sp. red fluorescent protein. *Nat Biotechnol* 2004, 22:1567–1572.
 42. Zamoyska R, Vollmer AC, Sizer KC, Liaw CW, Parnes JR. Two *Lyt-2* polypeptides arise from a single gene by alternative splicing patterns of mRNA. *Cell* 1985, 43:153–163.
 43. Liaw CW, Zamoyska R, Parnes JR. Structure, sequence, and polymorphism of the *Lyt-2T* cell differentiation antigen gene. *J Immunol* 1986, 137:1037–1043.
 44. Hancock JF, Cadwallader K, Paterson H, Marshall CJ. A CAAX or a CAAL motif and a second signal are sufficient for plasma membrane targeting of ras proteins. *EMBO J* 1991, 10:4033–4039.
 45. Jiang W, Hunter T. Analysis of cell-cycle profiles in transfected cells using a membrane-targeted GFP. *Biotechniques* 1998, 24:349–350 352, 354.
 46. Kay JN, Roeser T, Mumm JS, Godinho L, Mrejeru A, Wong RO, Baier H. Transient requirement for ganglion cells during assembly of retinal synaptic layers. *Development* 2004, 131:1331–1342.
 47. Kalderon D, Roberts BL, Richardson WD, Smith AE. A short amino acid sequence able to specify nuclear location. *Cell* 1984, 39:499–509.
 48. Emery G, Hutterer A, Berdnik D, Mayer B, Wirtz-Peitz F, Gaitan MG, Knoblich JA. Asymmetric Rab 11 endosomes regulate delta recycling and specify cell fate in the *Drosophila* nervous system. *Cell* 2005, 122:763–773.
 49. Rizzuto R, Brini M, Pizzo P, Murgia M, Pozzan T. Chimeric green fluorescent protein as a tool for visualizing subcellular organelles in living cells. *Curr Biol* 1995, 5:635–642.
 50. Shaner NC, Steinbach PA, Tsien RY. A guide to choosing fluorescent proteins. *Nat Methods* 2005, 2:905–909.
 51. Mahou P, Zimmerley M, Loulier K, Matho KS, Labroille G, Morin X, Supatto W, Livet J, Debarre

- D, Beaurepaire E. Multicolor two-photon tissue imaging by wavelength mixing. *Nat Methods* 2012, 9:815–818.
52. Hama H, Kurokawa H, Kawano H, Ando R, Shimogori T, Noda H, Fukami K, Sakaue-Sawano A, Miyawaki A. Scale: a chemical approach for fluorescence imaging and reconstruction of transparent mouse brain. *Nat Neurosci* 2011, 14:1481–1488.
53. Chung K, Deisseroth K. CLARITY for mapping the nervous system. *Nat Methods* 2013, 10:508–513.
54. Badaloni A, Bonanomi D, Albieri I, Givogri I, Bongarzone E, Valtorta F, Consalez GG. Transgenic mice expressing a dual, CRE-inducible reporter for the analysis of axon guidance and synaptogenesis. *Genesis* 2007, 45:405–412.
55. Feinberg EH, Vanhoven MK, Bendesky A, Wang G, Fetter RD, Shen K, Bargmann CI. GFP Reconstitution Across Synaptic Partners (GRASP) defines cell contacts and synapses in living nervous systems. *Neuron* 2008, 57:353–363.
56. Gordon MD, Scott K. Motor control in a Drosophila taste circuit. *Neuron* 2009, 61:373–384.
57. Han C, Jan LY, Jan YN. Enhancer-driven membrane markers for analysis of nonautonomous mechanisms reveal neuron-glia interactions in Drosophila. *Proc Natl Acad Sci USA* 2011, 108:9673–9678.
58. Brand AH, Perrimon N. Targeted gene expression as a means of altering cell fates and generating dominant phenotypes. *Development* 1993, 118:401–415.
59. Hayashi S, Ito K, Sado Y, Taniguchi M, Akimoto A, Takeuchi H, Aigaki T, Matsuzaki F, Nakagoshi H, Tanimura T, et al. GETDB, a database compiling expression patterns and molecular locations of a collection of Gal4 enhancer traps. *Genesis* 2002, 34:58–61.
60. Pfeiffer BD, Jenett A, Hammonds AS, Ngo TT, Misra S, Murphy C, Scully A, Carlson JW, Wan KH, Lavery TR, et al. Tools for neuroanatomy and neurogenetics in Drosophila. *Proc Natl Acad Sci USA* 2008, 105:9715–9720.
61. Jenett A, Rubin GM, Ngo TT, Shepherd D, Murphy C, Dionne H, Pfeiffer BD, Cavallaro A, Hall D, Jeter J, et al. A GAL4-driver line resource for Drosophila neurobiology. *Cell Rep* 2012, 2:991–1001.
62. Kvon EZ, Kazmar T, Stampfel G, Yanez-Cuna JO, Pagani M, Schernhuber K, Dickson BJ, Stark A. Genome-scale functional characterization of Drosophila developmental enhancers in vivo. *Nature* 2014, 512:91–95.
63. Lee T, Luo L. Mosaic analysis with a repressible cell marker for studies of gene function in neuronal morphogenesis. *Neuron* 1999, 22:451–461.
64. McGuire SE, Mao Z, Davis RL. Spatiotemporal gene expression targeting with the TARGET and gene-switch systems in Drosophila. *Sci STKE* 2004, 220:pl6.
65. Lai SL, Lee T. Genetic mosaic with dual binary transcriptional systems in Drosophila. *Nat Neurosci* 2006, 9:703–709.
66. Pfeiffer BD, Ngo TT, Hibbard KL, Murphy C, Jenett A, Truman JW, Rubin GM. Refinement of tools for targeted gene expression in Drosophila. *Genetics* 2010, 186:735–755.
67. Potter CJ, Tasic B, Russler EV, Liang L, Luo L. The Q system: a repressible binary system for transgene expression, lineage tracing, and mosaic analysis. *Cell* 2010, 141:536–548.
68. Golic KG, Lindquist S. The FLP recombinase of yeast catalyzes site-specific recombination in the Drosophila genome. *Cell* 1989, 59:499–509.
69. Branda CS, Dymecki SM. Talking about a revolution: the impact of site-specific recombinases on genetic analyses in mice. *Dev Cell* 2004, 6:7–28.
70. Griffin R, Binari R, Perrimon N. Genetic odyssey to generate marked clones in Drosophila mosaics. *Proc Natl Acad Sci USA* 2014, 111:4756–4763.
71. Gaj T, Sirk SJ, Barbas CF 3rd. Expanding the scope of site-specific recombinases for genetic and metabolic engineering. *Biotechnol Bioeng* 2014, 111:1–15.
72. Lee G, Saito I. Role of nucleotide sequences of loxP spacer region in Cre-mediated recombination. *Gene* 1998, 216:55–65.
73. McLeod M, Craft S, Broach JR. Identification of the crossover site during FLP-mediated recombination in the *Saccharomyces cerevisiae* plasmid 2 microns circle. *Mol Cell Biol* 1986, 6:3357–3367.
74. Senecoff JF, Cox MM. Directionality in FLP protein-promoted site-specific recombination is mediated by DNA-DNA pairing. *J Biol Chem* 1986, 261:7380–7386.
75. Schlake T, Bode J. Use of mutated FLP recognition target (FRT) sites for the exchange of expression cassettes at defined chromosomal loci. *Biochemistry (Mosc)* 1994, 33:12746–12751.
76. Larsen C, Franch-Marro X, Hartenstein V, Alexandre C, Vincent JP. An efficient promoter trap for detection of patterned gene expression and subsequent functional analysis in Drosophila. *Proc Natl Acad Sci USA* 2006, 103:17813–17817.
77. Vozizyanov Y, Konieczka JH, Stewart AF, Jayaram M. Stepwise manipulation of DNA specificity in FLP recombinase: progressively adapting FLP to individual and combinatorial mutations in its target site. *J Mol Biol* 2003, 326:65–76.
78. Thorpe HM, Wilson SE, Smith MC. Control of directionality in the site-specific recombination system of the *Streptomyces* phage phiC31. *Mol Microbiol* 2000, 38:232–241.
79. Groth AC, Olivares EC, Thyagarajan B, Calos MP. A phage integrase directs efficient site-specific integration in human cells. *Proc Natl Acad Sci USA* 2000, 97:5995–6000.

80. Siegal ML, Hartl DL. Transgene Coplacement and high efficiency site-specific recombination with the Cre/loxP system in *Drosophila*. *Genetics* 1996, 144:715–726.
81. Golic KG. Site-specific recombination between homologous chromosomes in *Drosophila*. *Science* 1991, 252:958–961.
82. Struhl G, Basler K. Organizing activity of wingless protein in *Drosophila*. *Cell* 1993, 72:527–540.
83. Duffy JB, Harrison DA, Perrimon N. Identifying loci required for follicular patterning using directed mosaics. *Development* 1998, 125:2263–2271.
84. Le X, Langenau DM, Keefe MD, Kutok JL, Neuberg DS, Zon LI. Heat shock-inducible Cre/Lox approaches to induce diverse types of tumors and hyperplasia in transgenic zebrafish. *Proc Natl Acad Sci USA* 2007, 104:9410–9415.
85. Nern A, Pfeiffer BD, Svoboda K, Rubin GM. Multiple new site-specific recombinases for use in manipulating animal genomes. *Proc Natl Acad Sci USA* 2011, 108:14198–14203.
86. Venken KJ, Bellen HJ. Emerging technologies for gene manipulation in *Drosophila melanogaster*. *Nat Rev Genet* 2005, 6:167–178.
87. Anastassiadis K, Glaser S, Kranz A, Berhardt K, Stewart AF. A practical summary of site-specific recombination, conditional mutagenesis, and tamoxifen induction of CreERT2. *Methods Enzymol* 2010, 477:109–123.
88. Huang J, Zhou W, Dong W, Watson AM, Hong Y. Directed, efficient, and versatile modifications of the *Drosophila* genome by genomic engineering. *Proc Natl Acad Sci USA* 2009, 106:8284–8289.
89. Heidmann D, Lehner CF. Reduction of Cre recombinase toxicity in proliferating *Drosophila* cells by estrogen-dependent activity regulation. *Dev Genes Evol* 2001, 211:458–465.
90. Venken KJ, He Y, Hoskins RA, Bellen HJ. P[acman]: a BAC transgenic platform for targeted insertion of large DNA fragments in *D. melanogaster*. *Science* 2006, 314:1747–1751.
91. Bischof J, Maeda RK, Hediger M, Karch F, Basler K. An optimized transgenesis system for *Drosophila* using germ-line-specific phiC31 integrases. *Proc Natl Acad Sci USA* 2007, 104:3312–3317.
92. Venken KJ, Schulze KL, Haelterman NA, Pan H, He Y, Evans-Holm M, Carlson JW, Levis RW, Spradling AC, Hoskins RA, et al. MiMIC: a highly versatile transposon insertion resource for engineering *Drosophila melanogaster* genes. *Nat Methods* 2011, 8:737–743.
93. Dietzl G, Chen D, Schnorrer F, Su KC, Barinova Y, Fellner M, Gasser B, Kinsey K, Oettel S, Scheiblaue S, et al. A genome-wide transgenic RNAi library for conditional gene inactivation in *Drosophila*. *Nature* 2007, 448:151–156.
94. St Johnston D. Using mutants, knockdowns, and transgenesis to investigate gene function in *Drosophila*. *WIREs Dev Biol* 2013, 2:587–613.
95. Akitake CM, Macurak M, Halpern ME, Goll MG. Transgenerational analysis of transcriptional silencing in zebrafish. *Dev Biol* 2011, 352:191–201.
96. Card JP, Kobiler O, McCambridge J, Ebdlahad S, Shan Z, Raizada MK, Sved AF, Enquist LW. Microdissection of neural networks by conditional reporter expression from a Brainbow herpesvirus. *Proc Natl Acad Sci USA* 2011, 108:3377–3382.
97. Chen F, LoTurco J. A method for stable transgenesis of radial glia lineage in rat neocortex by piggyBac mediated transposition. *J Neurosci Methods* 2012, 207:172–180.
98. Garcia-Marques J, Lopez-Mascaraque L. Clonal identity determines astrocyte cortical heterogeneity. *Cereb Cortex* 2013, 23:1463–1472.
99. Timofeev K, Joly W, Hadjiconomou D, Salecker I. Layered netrins act as positional cues to control layer-specific targeting of photoreceptor axons in *Drosophila*. *Neuron* 2012, 75:80–93.
100. Oliva C, Choi CM, Nicolai LJ, Mora N, De Geest N, Hassan BA. Proper connectivity of *Drosophila* motion detector neurons requires Atonal function in progenitor cells. *Neural Dev* 2014, 9:4.
101. von Hilchen CM, Bustos AE, Giangrande A, Technau GM, Altenhein B. Predetermined embryonic glial cells form the distinct glial sheaths of the *Drosophila* peripheral nervous system. *Development* 2013, 140:3657–3668.
102. Di Girolamo N, Bobba S, Raviraj V, Delic NC, Slatetova I, Nicovich PR, Halliday GM, Wakefield D, Whan R, Lyons GJ. Tracing the fate of limbal epithelial progenitor cells in the murine cornea. *Stem Cells* 2014. doi:10.1002/stem.1769.
103. Szymczak-Workman AL, Vignali KM, Vignali DA. Design and construction of 2A peptide-linked multicistronic vectors. *Cold Spring Harb Protoc* 2012, 2012:199–204.